isobars close to vertical. However, there is a clockwise skewing of these isobars, which is consistent with a weak induced circulatory motion at the upper half of the inlet. This was implied in the vorticity distributions given by the calculations, as in Figs. 7-11 of Ref. 1.

In the lower part of the inlet, there is a substantial region of lower stagnation pressure. This ocurs in the neighborhood of the inlet vortex. The cross-plane velocities in this region are also considerably higher, the measurements showing values up to almost half the streamwise velocities. The position of the inlet vortex core is offset about 25 deg from the vertical (i.e., is at roughly "five o'clock"). This shift is associated with the induced velocity field of the inlet vortex in the presence of solid boundaries.

A map of the axial component of vorticity in the inlet, computed from the measured velocity, is shown in Fig. 4. Contours of ω_x/ω_∞, the local axial vorticity nondimensionalized by the upstream value, are plotted in the figure. Note that obtaining the vorticity involves, in some regions, the difference of two large velocities. In addition, for this flow, the vorticity is not a monotonically varying quantity, but rather varies strongly over the face. Thus, although the central features shown in Fig. 4 are unambiguous, some of the details should be viewed with this in mind.

Several features are apparent. First, as expected, the inlet vortex is a region of high vorticity due to vortex stretching. Also, because the vorticity varies so strongly over the face, the assigning of "a" circulation to the inlet vortex is somewhat arbitrary. However, we have computed the circulation around various contours to obtain several measures of this quantity and, based on these results, a reasonable value of the inlet vortex circulation for the present configuration (i.e., specified H/D, U_i/U_c), normalized by the upstream vorticity and capture area cross section, A_∞ ($A_\infty = U_i A_i/U_c$, where A_i is the inlet area), is

$$\frac{\Gamma}{\omega_\infty A_\infty} = \frac{\Gamma}{\omega_\infty U_i A_i/U_c} \simeq 2$$

As far as the authors are aware, this is the first time a measurement of this quantity has been made.

A second feature is a region of high vorticity of the opposite sign (from that associated with the inlet vortex) above and to the left of the inlet vortex. This marks the other leg of (or some of) the ingested vortex lines, the lower parts of which form the core of the inlet vortex. As shown in the calculations in Ref. 1, there should be substantial stretching of these opposite-sign vortex filaments in the region below the inlet centerline; this is seen in the data. What was not seen, however, is the large magnitude of this opposite-sign vorticity, as well as its nonsymmetric distribution—both of which are results of the mutual induction of the two opposite legs and the interaction with the solid boundaries. These effects, which are associated with the nonlinearity of the problem, are not included in the calculations.

The third feature is the weak circulation in the upper half of the inlet, again of the opposite sign from the inlet vortex as predicted by the calculations, although no real quantitative comparisons can be made because of the level of uncertainty in the data.

Summary and Conclusion

Measurements have been carried out to illustrate the nature of an inlet vortex in a flow with a vertical component of ambient vorticity. It is the amplification of this vorticity (by stretching) as the vortex lines are drawn into the inlet that is responsible for the vortex formation. Features of the amplification shown by the velocity measurements inside the inlet are a strong vortex, associated with the ground leg, at the lower part of the inlet at roughly "five o'clock" and, immediately above and to the left, a region of high vorticity of the opposite sign. The latter marks the other leg of the ingested vortex lines. The experiments show qualitative agreement with calculations based on a secondary flow approach,[1] although there are differences due to the nonlinear effects that occur in the actual phenomenon.

Acknowledgment

This work was sponsored by the Air Force Office of Scientific Research under Contract F49620-82-K-0002, Dr. J.D. Wilson, Program Manager.

References

[1]De Siervi, F., Viguier, H.C., Greitzer, E.M., and Tan, C.S., "Mechanisms of Inlet Vortex Formation," *Journal of Fluid Mechanics*, Vol. 124, 1982, pp. 173-207.

[2]Liu, W., "Design and Analysis of an Experimental Facility for Inlet Vortex Investigation," Gas Turbine Lab., Massachusetts Institute of Technology, Cambridge, Rept. 166, 1982.

[3]Whitfield, C.E., Kelley, J.C., and Barry, B., "A Three-Dimensional Analysis of Rotor Wakes," *Aeronautical Quarterly*, Vol. 23, Nov. 1972, pp. 285-300.

[4]Schmidt, D.P. and Okiishi, T.H., "Multistage Axial-Flow Turbomachine Wake Production, Transport and Interaction," *AIAA Journal*, Vol. 15, Aug. 1977, pp. 1138-1145.

[5]Shin, H.W. and Shippee, C., "Quantitative Investigation of Inlet Vortex Flow Field," Gas Turbine Lab., Massachusetts Institute of Technology, Rept. 179, March 1984.

Turbulent Boundary-Layer Wall Pressure Fluctuations Downstream of a Tandem LEBU

George B. Beeler*
NASA Langley Research Center, Hampton, Virginia

Nomenclature

C_f	= skin-friction coefficient = τ/q_∞
d^+	= effective transducer diameter scaled by wall units dU_τ/ν
h	= height of LEBU from splitter plate
p'_w	= rms wall pressure fluctuation
q_∞	= freestream dynamic pressure
U_∞	= freestream velocity
U_τ	= skin-friction velocity = $\sqrt{\tau/\rho}$
x	= streamwise coordinate
x_0	= location of δ_0 and first LEBU
δ_0	= initial turbulent boundary-layer thickness
δ^*	= displacement thickness
$\phi(\omega)$	= power spectral density of p'_w
τ	= wall shear stress
ρ	= density
ν	= kinematic viscosity
ω	= circular frequency

Introduction

TURBULENT wall pressure fluctuations (p'_w) are a source of noise and inaccuracy for passive SONAR.[1] The injection of polyethylene oxide or certain other polymers into the turbulent boundary layer reduces p'_w in water,[2] but requires

Received July 6, 1984; revision received July 22, 1985. This paper is declared a work of the U.S. Government and is not subject to copyright protection in the United States.

*Aerospace Engineer, Viscous Flow Branch, High-Speed Aerodynamic Division. Member AIAA.

injectors and storage volume to carry the polymer. On CTOL aircraft, turbulent wall pressure fluctuations act to excite fuselage vibrations.[3] In order to reduce consequent cabin noise, absorbant material is often added to the fuselage with an associated weight penalty. For the air case, p_w' is typically left "untreated." Therefore, the reduction of turbulent boundary-layer wall pressure fluctuations would be very beneficial.

Recent research has revealed that two rigid ribbons mounted in tandem and immersed in a turbulent boundary layer yield a net drag reduction 0 (10%) (see Ref. 4 and references cited therein). These ribbons are called large-eddy breakup devices (LEBUs). The LEBUs lower the downstream skin-friction coefficient up to 25%. The present experiment was performed to determine if the drag reduction is accompanied by a corresponding reduction in turbulent boundary-layer wall pressure fluctuations.

Experiment

The experiment was performed in the 2′ × 3′ boundary-layer channel at NASA Langley Research Center. This facility is a closed-circuit air tunnel with a 6.1 m long tunnel test section. The flow passes through a section of honeycomb and four screens to reduce the freestream turbulence. The test section is fitted with a splitter plate to aid in obtaining a nominally zero pressure gradient boundary layer. The splitter plate and test conditions are shown in Fig. 1 and Table 1. The location of the transducer was near the point of maximum C_f reduction [0 (25%)] 1.52 m from the leading edge of the splitter plate.[4] This point was selected to facilitate mounting the transducer and to be near the maximum effect of the tandem LEBUs. The fan noise and device noise were not muffled and not measured. However, fan noise in this facility is low frequency [0 (100 Hz)] and does not appear to affect the significance of the present measurement.

The transducer used was a Bruel and Kjaer 4138 microphone. In order to measure the effect on scales smaller than 3.175 mm ($f \simeq 12$ kHz), the microphone was fitted with a pinhole cap (effective diameter 0.5 mm). Although pinhole microphones have been shown to produce results that differ from piezoelectric transducers, the comparative nature of the present measurement allows valid conclusions to be drawn. The microphone arrangement has a resonant point well above the measured frequencies. The signal from the microphone was low-pass-filtered with 3 dB point at 22 kHz. This provided a frequency range of 0-20 kHz. The signal was acquired on an HP-3580 spectrum analyzer. The resolution of the measurement was 100 Hz, which places the fan noise in the lowest 5 points of the spectra.

The effect of the tandem LEBUs was determined by first measuring and verifying the reference plate spectra (without the LEBU devices). Then the tandem LEBUs were installed and the spectra were taken again. The vibrational components of these measurements were obtained by acquiring the spectra with the microphone covered.

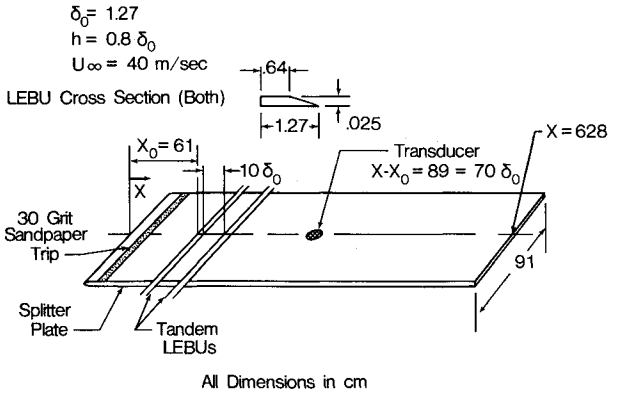

Fig. 1 Experiment arrangement.

Results

The nondimensional power spectra obtained are shown in Fig. 2 along with data from Ref. 5. Figure 2 indicates the match of the flat plate data with similar measurements ($d^+ = 40.6$-46.8 for the present experiment). Note that the LEBU modified boundary layer does not scale to the unmodified boundary layer much beyond $\omega\nu/U_\tau^2 > 0.3$. This indicates a net reduction in p_w' over the unmodified boundary layer (since U_τ has been reduced by the LEBUs). The $\phi(\omega)$ reduction from 7-8 kHz is of the same order as the C_f reduction (25%) due to the tandem LEBUs. This measurement suggests that the reduction in p_w' is due to a shift in flow structure size, and this hypothesis is supported by the work of Refs. 6 and 7. However, a corresponding reduction of $\phi(\omega)$ in the low-frequency range is not seen. This is probably due to masking of any reductions by tunnel noise in conjunction with vibration.

In Fig. 3 the spectra are presented in dimensional form with the vibration data to illustrate the lack of effect that the LEBUs have on the high-frequency portion of the power spec-

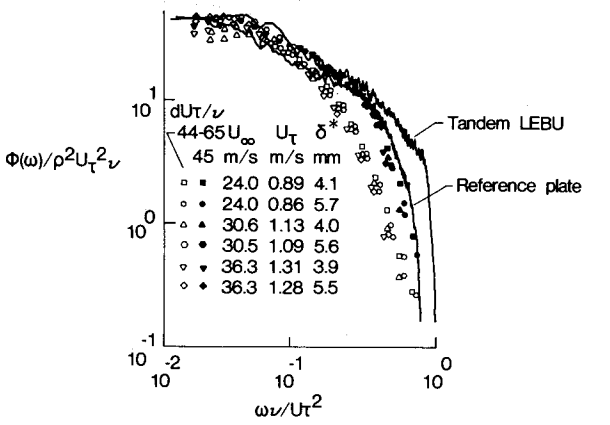

Fig. 2 Nondimensional power spectra of reference plate, and reference plate with tandem LEBUs.

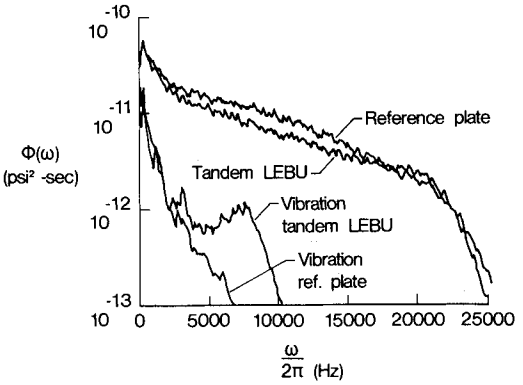

Fig. 3 Dimensional power spectra of reference plate, reference plate with tandem LEBUs, and vibration.

Table 1 Transducer location flow characteristics

At transducer reference plate	With LEBU
$\delta^* = 0.3526$ cm	$\delta^* = 0.3505$ cm
$\theta = 0.2598$ cm	$\theta = 0.2545$ cm
$C_f = 0.00281$	$C_f = 0.00224$
$d^+ = 46.8$	$d^+ = 40.6$
$U_\tau = 1.5$ m/s	$U_\tau = 1.3$ m/s

tra (this is difficult to discern from Fig. 2). This could be due to the use of the pinhole microphone (as suggested by Ref. 8). However, the effect of the tandem LEBUs is seen in the lower part of the region where the pinhole and piezoelectric transducer measurements differ. These data show a net reduction of p_w' of 12.5%. It is noted that LEBU device noise could be another source of error in the high-frequency $\phi(\omega)$ measured (due to dynamic flow separation on the LEBUs). Notice that vibration does not affect the measurement significantly in the region of the measured effects.

Conclusions

An initial measurement of p_w' downstream of tandem LEBUs show a significant reduction compared to the reference flat plate case. The average magnitude of the p_w' reduction is 12.5%. The peak reduction is at 7-8 kHz and is on the order of the C_f reduction due to the tandem LEBUs (25%). Since the measurement is at only one location, device noise and other effects (such as downstream extent/relaxation) could not be evaluated. These data provide an indication of a secondary benefit of LEBUs (in addition to their skin-friction reduction performance).

References

[1]Urick, R., *Principles of Underwater Sound*, 3rd ed., McGraw-Hill Book Co., New York, 1983, p. 365.

[2]Greshilov, E.M., Evtushenko, A.V., and Lyamshev, L.M., "Hydrodynamic Noise and Toms Effect," *Soviet Physics - Acoustics*, Vol. 21, No. 3, 1975, pp. 396-404.

[3]Bhat, W.V. and Wilby, J.B., "Interior Noise Radiated by an Airplane Fuselage Subjected to Turbulent Boundary Layer Excitation and Evaluation of Noise Reduction Treatments," *Journal of Sound and Vibration*, Vol. 18, No. 4, 1971, pp. 449-454.

[4]Anders, J.B., Hefner, J.N., and Bushnell, D.M., "Performance of Large-Eddy Breakup Devices at Post Transition Reynolds Numbers," AIAA Paper 84-0345, Jan. 1984.

[5]Thomas, A.S.W., "Organized Structures in the Turbulent Boundary Layer," Ph.D. Dissertation, University of South Adelaide, Australia, 1977.

[6]Hefner, J.N., Weinstein, L.M., and Bushnell, D.M., "Large-Eddy Breakup Scheme for Turbulent Viscous Drag Reduction," *Progress in Astronautics and Aeronautics: Viscous Flow Drag Reduction*, Vol. 72, edited by Gary R. Hough, AIAA, New York, 1981, pp. 118-127.

[7]Hefner, J.N., Anders, J.B., and Bushnell, D.M., "Alteration of Outer Flow Structures for Turbulent Drag Reduction," AIAA Paper 83-0293, Jan. 1983.

[8]Bull, M.K. and Thomas, A.S.W., "High Frequency Wall Pressure Fluctuations in Turbulent Boundary Layers," *Physics of Fluids*, Vol. 19, April 1976, pp. 597-599.

Quasilinear Form of Rankine-Hugoniot Jump Conditions

Czeslaw P. Kentzer*
Purdue University, West Lafayette, Indiana

THIS Note shows that the generalized Rankine-Hugoniot jump conditions associated with the divergence (or "conservative") form of the Euler equations of gasdynamics may be put in the equivalent form corresponding to the quasilinear (or "nonconservative") form. Associating a proper set of algebraic jump conditions directly with a given set of differential equations is crucial in numerical computations according to Lax,[1] and may be conveniently formalized using Emde's notation,[2] namely, associating a volume (differential) operator with an appropriate surface (algebraic) multiplication operator. In computational gasdynamics the usefulness of such an association goes beyond mere notation. This is so because finite approximations may be viewed as algebraic operators replacing (approximating) differential operators and may be chosen so as to collapse automatically to the correct jump conditions in the presence of discontinuities. This property of finite difference schemes was demonstrated earlier[3] for the case of the divergence form of the Euler system. Here we demonstrate the technique of obtaining the quasilinear jump conditions corresponding to a given quasilinear form of the Euler system. The intention is to publicize the possibilities of constructing difference schemes approximating simultaneously the differential equations and the jump conditions for all forms of the Euler system of gasdynamics.

We shall start with the divergence form of the Euler equations,

$$\frac{\partial \rho}{\partial t}+\nabla\cdot(\rho \boldsymbol{u})=0, \qquad \frac{\partial \rho \boldsymbol{u}}{\partial t}+\nabla\cdot(\rho \boldsymbol{u}\boldsymbol{u})+\nabla p=0$$

$$\frac{\partial \rho e^{\circ}}{\partial t}+\nabla\cdot(\rho h^{\circ}\boldsymbol{u})=0 \tag{1}$$

where ρ is the mass density, $\boldsymbol{u}$ the velocity, p the pressure, e° the total specific internal energy, and $h^{\circ}=e^{\circ}+p/\rho$ the total specific enthalpy.

Equation (1) allows for the use of Emde's notation, namely, in the presence of a surface of discontinuity Σ, the differential system (1) must be replaced by an algebraic system formally obtained from the first by replacing volume differential operators $\partial/\partial t$ and ∇ by the surface algebraic multiplication operators $-U$ and $\boldsymbol{n}$, respectively, which operate on the differences (jumps) in the differentiated functions across the singular surface. The jumps are surface functions, i.e., functions of position on Σ. Thus, using Emde's notation, we obtain from Eq. (1) the known result (see, e.g., Ref. 4), namely,

$$-U[\rho]+\boldsymbol{n}\cdot[\rho \boldsymbol{u}]=0, \qquad -U[\rho \boldsymbol{u}]+\boldsymbol{n}\cdot[\rho \boldsymbol{u}\boldsymbol{u}]+\boldsymbol{n}[p]=0$$

$$-U[\rho e^{\circ}]+\boldsymbol{n}\cdot[\rho h^{\circ}\boldsymbol{u}]=0 \tag{2}$$

where $\boldsymbol{n}$ is the unit spatial normal to the discontinuity, U the displacement speed of the discontinuity in the direction of $\boldsymbol{n}$, and $[\psi]=\psi_2-\psi_1$ is the jump in ψ across the surface Σ.

Quasilinear forms of the Euler system of gasdynamics may be obtained directly from the divergence form [Eq. (1)] by applying rules for the derivatives of products, subtraction of multiples of mass or momentum equations, and rearrangement of terms. We shall perform parallel operations on the algebraic jump conditions (2). For this we need the following:

$$[ab]=a_2b_2-a_1b_1$$

$$=a_2b_2-a_2b_1+a_2b_1-a_1b_1=a_2[b]+b_1[a]$$

$$=a_2b_2-a_1b_2+a_1b_2-a_1b_1=a_1[b]+b_2[a]$$

Preferring expressions symmetric in subscripts, we average and write

$$[ab]=\langle a\rangle[b]+\langle b\rangle[a]$$

where $\langle a\rangle=(a_2+a_1)/2=$ the arithmetic average of a. Note the analogy of the above to the formula $\delta(ab)=a\delta(b)+b\delta(a)$. We will need also the geometric mean, defined as

Received June 17, 1985.

*Associate Professor of Aeronautics and Astronautics. Member AIAA.